Theoretical Study on Reactions of HO_2 Radical with Photodissociation Products of Cl_2SO (ClSO and SO)

Milan Szori,[†] Imre G. Csizmadia,[†,‡] Christa Fittschen,[§] and Bela Viskolcz*

Department of Chemical Informatics, Faculty of Education, University of Szeged, Szeged, Boldogasszony sgt. 6. Hungary 6725, Department of Chemistry, University of Toronto, Toronto ON, Canada M5S 3H6, and PhysicoChimie des Processus de Combustion et de l'Atmosphère, UMR CNRS 8522, Université des Sciences et Technologies de Lille 1, 59655 Villeneuve d'Ascq Cedex, France

Received: February 9, 2009; Revised Manuscript Received: July 11, 2009

The possible reactions of HO_2 radical with the intermediates of the Cl_2SO photolysis (ClSO and SO) were studied using G3MP2//B3LYP/cc-pVTZ+d level of theory and Martin's W1U method. For the reaction between HO_2 and ClSO radicals, the following mechanisms are supposed to be the main reaction pathways

$$HO_2 + ClSO \rightarrow {}^3HOO \times ClSO \rightarrow HOO(Cl)SO \rightarrow OH + ClSO_2 \rightarrow HO + Cl + SO_2$$

$$HO_2 + ClSO \rightarrow {}^3HOO \times ClSO \rightarrow HOO(Cl)SO \rightarrow OH + ClSO_2 \rightarrow HO(Cl)SO_2$$

On the basis of G3MP2//B3LYP/cc-pVTZ+d and highly accurate W1U calculations, the reaction of HOO with ^3SO species has also been explored, and the following dominant consecutive reactions may describe the fast oxygen transfer

$$HO_2 + {}^3SO \rightarrow {}^4HOO \times SO \rightarrow {}^2HOOSO \rightarrow OH + SO_2$$

In both reaction mechanisms, the first step is a barrierless formation of relatively stable van der Waals complexes that lead via intersystem crossing to intermediate adducts. Thermodynamically favored decomposition products of ^2HOOSO are OH radical and SO_2. In the case of the ClSO and HO_2 reaction, the dissociation of HOO(Cl)SO resulted in OH and $ClSO_2$. Further decomposition of $ClSO_2$ to Cl atom and SO_2 competes with formation of $HO(Cl)SO_2$ via OH addition reaction to $ClSO_2$. We also report on high-level quantum chemical calculation (W1U) to predict values for the heat of formation of $^2HSO_3$, ^2HOOSO, and $^2OOS(H)O$ radicals using the most reliable thermodynamic data of OH and SO_3: $\Delta_f H^{298.15K}(^2HSO_3) = -256.2$ kJ/mol, $\Delta_f H^{298.15K}(^2HOOSO) = -152.6$ kJ/mol, and $\Delta_f H^{298.15K}(^2OOS(H)O) = -8.3$ kJ/mol. On the basis of W1U standard reaction enthalpy for the reaction $ClSO + HOO \rightarrow HCl + SO_3$, the heat of formation for the ClSO radical was also computed to be $\Delta_f H^{298.15K}(ClSO) = 102.6$ kJ/mol within 4 kJ mol^{-1} error.

1. Introduction

Thionyl chloride, Cl_2SO, is a potentially good Cl-atom precursor for laser photolysis studies because of its two chlorine atoms and its high absorption cross section in the UV spectral range below 300 nm. At classical laser wavelengths (193, 248, or 266 nm), the cross sections of thionyl chloride are more than one order of magnitude higher than those of other commonly used chlorine atom precursors such as Cl_2, phosgene $COCl_2$, or oxalyl chloride $(COCl)_2$.[1]

Many studies have been published on the photodissociation of Cl_2SO[2−7] and there is a general agreement on the important dissociation channels

molecular channel

$$Cl_2SO + h\nu \rightarrow SO + Cl_2 \quad \lambda_{thr} = 557.1 \text{ nm} \qquad (1a)$$

radical channel

$$\rightarrow ClSO + Cl/Cl^* \quad \lambda_{thr} = 499.8 \text{ nm} \qquad (1b)$$

three body channel

$$\rightarrow SO + 2Cl/Cl^* \quad \lambda_{thr} = 263.5 \text{ nm} \qquad (1c)$$

The threshold wavelengths, λ_{thr}, are taken from Chichinin et al.[7] Chlorine atoms can be formed in two electronic states, namely, $Cl(^2P_{3/2})$ and $Cl^*(^2P_{1/2})$. The photolysis of Cl_2SO at 248 nm also simultaneously excites the species to two states, $2^1A'$ and $2^1A''$, the latter being the main pathway and generating internally excited ClSO radicals and $Cl(^2P_{1/2})$ atoms. Excitation to the A′ state is a

* Corresponding author. Fax: +36 62 420 953. E-mail: viskolcz@jgypk.u-szeged.hu.
[†] University of Szeged.
[‡] University of Toronto.
[§] Université des Sciences et Technologies de Lille 1.

10.1021/jp901183k CCC: $40.75
Published on Web 08/20/2009

minor path and leads to the formation of ground-state SO and two Cl-atoms. Depending on the total pressure, excited ClSO radical can be stabilized by collision,[8] and it is also able to undergo unimolecular decay into SO and Cl atoms.[9]

Chlorine atoms produced by the above-mentioned photodissociation processes are able to generate the hydroperoxyl radical rapidly in the presence of CH_3OH and O_2 via the following mechanism

$$Cl + CH_3OH \rightarrow CH_2OH + HCl \quad k_2^{298K} = 5.5 \times 10^{-11} \tag{2}$$

$$CH_2OH + O_2 \rightarrow CH_2O + HO_2 \quad k_3^{298K} = 9.7 \times 10^{-12} \tag{3}$$

The rate constants, k_2 and k_3 (in cm^3 $molecule^{-1}$ s^{-1}) are taken from the work of Atkinson et al.[10] To use Cl_2SO laser photolysis in the presence of methanol, CH_3OH, and O_2 as a suitable HO_2 source, other possibly obscure reactions need to be explored. In a recent work, we have investigated the formation of CH_2O following the photolysis of Cl_2SO in the presence of CH_3OH and O_2: a very fast primary formation of CH_2O was followed by a slow, secondary formation of CH_2O, depending in rate and yield on the concentrations of the different species. These findings have been interpreted by reactions of the byproduct of the Cl_2SO photolysis, SO and ClSO, with HO_2.[1] To the best of our knowledge, there is no information available on the fate and reactivity of these stabilized photodissociation products. This was the motivation for us to investigate the following two reaction systems by means of ab initio calculation

$$HO_2 + ClSO \rightarrow \text{products} \tag{4}$$

$$HO_2 + {}^3SO \rightarrow \text{products} \tag{5}$$

2. Computational Methods

All the geometries are obtained at the B3LYP/cc-pVTZ+d level of theory,[11−13] where +d indicates the addition to all second-row atoms of a single high-exponent d-type inner polarization function. For all transition states, an intrinsic reaction coordinate (IRC) calculation was performed to confirm that the transition state did indeed approach the correct minima. The calculated B3LYP/cc-pVTZ+d harmonic frequencies were scaled using a factor of 0.985, and then these scaled frequencies were used in the calculations of thermochemical properties. Furthermore, the modified G3MP2B3 scheme[14] (indicated as G3MP2//B3TZd) was computed using the optimized B3LYP/cc-pVTZ+d geometries. At this point, frequency calculation was also replaced by B3LYP/cc-pVTZ+d. Additionally, single-point quadratic configuration interaction calculations were performed in the frozen core approximation (FC) for the correlation calculation, QCISD(T,FC)/6-31G(d). Then, second-order Moeller−Plesset perturbation theory, MP2(FC), was performed with the basis sets 6-31G(d) and 6-311+G(2df,2p) on oxygen and 6-311+G(3d2f,2p) on sulfur and chlorine atoms, designated as G3MP2Large. (For the open shell species, the values of $<S^2>$ obtained at MP2(FC)/G3MP2Large are reported in the Supporting Information. They are only slightly affected by spin contamination, except for TS2 and TS5, where the effect is considerably high.) A spin−orbit correction is included for single atomic species. Last but not least, the higher level correction (HLC) takes into account remaining deficiencies in the energy calculations. Basically, G3MP2//B3TZd differs from G3MP2B3[14] in the replacement of B3LYP/6-31G(d) with the B3LYP/cc-pVTZ+d level of theory for geometry optimizations and for harmonic frequency calculations. Then, the standard G3MP2//B3TZd enthalpy ($H^{298.15K}$) can be given as follows

$$H^{298.15K} = E_{QCISD(T)/6-31G(d)} + E_{MP2/G3MP2Large} - E_{MP2/6-31G(d)} + H^{298.15K}_{corr,B3LYP/cc-pVTZ+d} + E_{HLC}$$

G3MP2//B3TZd calculations were carried out in the case of both reaction systems studied. To estimate the accuracy of the G3MP2//B3TZd calculations, we also used Martin's W1U composite method[15] to approximate infinite-basis-set CCSD(T) calculations, and it was used as a reference method for G3MP2//B3TZd.

The standard W1U procedure also uses B3LYP/cc-pVTZ+d-optimized geometries. CCSD and CCSD(T) calculations are then performed with basis sets of systematically increasing size (aug'-cc-pVDZ+2d and aug'-cc-pVnZ+2d1f, where n = T, Q; the characters of +2d1f indicate the addition of high exponent d and f functions to all second-row atoms).[15] We performed separate extrapolations to determine the SCF, CCSD valence correlation, and triple-excitation components of the total atomization energy at the basis-set limit. A two-point SCF extrapolation was used for W1U, as was recently proposed.[16] The W1U procedure includes contributions from core correlation, scaled ZPVE, scalar relativistic effects, and first-order spin−orbit coupling on molecules and atoms.

The relative energies of the intersystem crossings (ISCs) were estimated from a series of partial optimizations (1D scan) at the B3LYP/cc-pVTZ+d level of theory, where the distance between the terminal oxygen of HOO and the sulfur was kept fixed during the optimizations. The distance was systematically varied between 1.6 and 3.2 Å. These calculations were carried out on the singlet and the triplet potential surfaces in the case of HOO + ClSO as well as on the doublet and the quartet potential surfaces in the case of HOO + ^{3}SO. Additionally, not only was the energy corresponding to the electronic state used for the geometry optimization computed, but so was the other state's as a single-point calculation. For instance, this means that the energy of the lowest singlet state was also characterized on the geometry obtained by optimization in the triplet state in the case of HOO + ClSO. Although this methodology is not that accurate, it is able to estimate the necessary values for ISCs instead of having to obtain them via extremely computer-demanding multireference calculations.

A comparison of G3MP2//B3TZd, W1U, and experimental values was also made for the estimation of the reliability of G3MP2//B3TZd. All calculations have been performed using the Gaussian03 computer program.[17]

3. Results and Discussion

The possible reactions of HOO and ClSO are almost unknown, and only the dissociation and isomerization channels of $^2HOSO_2$ have been previously discussed.[18−22] In addition, calculations of thermochemical properties for sulfur- and oxygen-containing species are still challenges for computational methods.[23] However, the W1U method is limited only for either small molecules or highly symmetric species, but it is known as one of the most accurate (mean absolute deviation is ∼2 kJ mol^{-1}) composite methods.[24] Accordingly, this seems to be a reliable reference method for estimating the accuracy of the much faster G3MP2//B3TZd method. To do this, we had

TABLE 1: Comparison of Experimental Reaction Enthalpies in kJ mol^{-1} ($\Delta_r H^{298.15K}$) with Those of W1U and G3MP2//B3TZd Methods[a]

reaction	$\Delta_r H^{298.15K25}_{exptl}$ kJ mol^{-1}	$\Delta_r H^{298.15K}_{W1U}$ kJ mol^{-1}	$\Delta_r H^{298.15K}_{G3MP2//B3TZd}$ kJ mol^{-1}
$HCl + SO_3 \rightarrow HOCl + SO_2$	115.5	115.0 (0.5)	111.1 (4.4)
$HCl + SO_3 \rightarrow SO_2 + OH + Cl$	349.8	353.2 (−3.4)	336.3 (13.5)
$HCl + SO_3 \rightarrow ClSO + HOO$		398.1 (−)	379.2 (−)
$HCl + SO_3 \rightarrow HOSO_2 + Cl$	236.4	237.7 (−1.3)	232.8 (3.6)

[a] Deviations from the experimental data are listed in the parentheses.

compared G3MP2//B3TZd, W1U, and the available experimental heats of reaction in the case of $HO_2 + ClSO$ reaction (Table 1).

The W1U method performs quite well; the maximum absolute deviation is only 3.4 kJ mol^{-1}. The G3MP2//B3TZd results have larger maximum deviations (13.5 kJ mol^{-1}), but it still gives the possibility for fairly good enthalpy data for all reactions studied. The comparison of calculated and experimental heats of formation can also test the reliability of the computational methods.

Heat of Formation. On the basis of our theoretical results, the heats of formation of $^2HSO_3$, ^2HOOSO, $^2OOS(H)O$, and $^2HOSO_2$ can be calculated, and they are also compared with the available literature data.

Because the enthalpies of formation for hydrogen and sulfur trioxide are experimentally well known, they have been used as references in the calculation of the sulfuric compounds

$$H + SO_3 \rightarrow X \quad (6)$$

where X can be $^2HOSO_2$, ^2HOOSO, $^2HSO_3$, or $^2OOS(H)O$ molecule.

The heat of formation of molecule X, $\Delta_f H^{298.15K}_{theor}(X)$, is calculated as follows

$$\Delta_f H^{298.15K}_{theor}(X) = \{H^{298.15K}_{theor}(X) - [H^{298.15K}_{theor}(H) + H^{298.15K}_{theor}(SO_3)]\} + [\Delta_f H^{298.15K}_{exptl}(H) + \Delta_f H^{298.15K}_{exptl}(SO_3)]$$

where $H^{298.15K}_{theor}(X)$, $H^{298.15K}_{theor}(H)$, and $H^{298.15K}_{theor}(SO_3)$ are either G3MP2//B3TZd or W1U enthalpy values. $\Delta_f H^{298.15K}_{exptl}(H) = 217.998$ kJ mol^{-1} and the $\Delta_f H^{298.15K}_{exptl}(SO_3) = -395.753$ kJ mol^{-1} are the experimental heat of formation values from the ATcT database.[25] The thermochemical properties obtained from W1U and G3MP2//B3TZd as well as the literature data are listed in Table 2.

The heat of formation for $^2HOSO_2$ based on our W1U calculation (−376.6 kJ mol^{-1}) is in quite good agreement with experimental results recommended by Pilling and coworkers (−373.0 kJ mol^{-1})[19] (Table 2). A value of −374.1 kJ mol^{-1} recently published by Klopper et al.[18] is also consistent with our results. Whereas Somnitz[20] suggested a slightly less exothermic value of −368.8 kJ mol^{-1} from his G3X calculations, both Burcat[25] and Fulle[21] recommended a much more exothermic formation (−385.0 and −391.0 kJ mol^{-1}, respectively). As is shown in Table 2, the G2 enthalpy of $^2HOSO_3$[22] is almost identical to the value of Burcat (−386.7 kJ mol^{-1}).

TABLE 2: Calculated Thermochemical Properties for HSO_3 Isomers Using W1U and G3MP2//B3TZd Methods

species	$\Delta_f H^{298.15K}$ kJ mol^{-1}	$S^{298.15K}$ J mol^{-1} K^{-1}	ref
$^2HOSO_2$	−374.1 ± 3		Klopper[18]
	−376.6	288.8	this work (W1U)
	−373 ± 6		Pilling et al. (3rd Law)[19]
	−367.9	288.8	this work (G3MP2//B3TZd)
	−368.8		Somnitz (G3X)[20]
	−385.0	294.061	Burcat et al.[25]
	−391.0		Fulle et al.[21]
	−386.7		Li et al. (G2)[22]
^2HOOSO	−152.6	305.1	This work (W1U)
	−154.5	305.1	this work (G3MP2//B3TZd)
	−173.8		Li et al. (G2)[22]
$^2HSO_3$	−256.2	284.5	this work (W1U)
	−241.6	284.5	this work (G3MP2//B3TZd)
	−245.3		Li et al. (G2)[22]
$^2OOS(H)O$	−8.3	306.5	this work (W1U)
	−12.4	306.5	this work (G3MP2//B3TZd)

To the best of our knowledge, there are no experimental heat of formation data available for $^2HSO_3$, ^2HOOSO, and $^2OOS(H)O$ radicals. G3MP2//B3TZd and W1U heat of formation values are consistent with each other in the case of ^2HOOSO; however, the G2 result suggested by Li[22] is significantly smaller (by 21.2 kJ mol^{-1}). For the $^2HSO_3$ species, the G2 heat of formation is close to our G3MP2//B3TZd value, but the largest deviation of G3MP2//B3TZd (−241.6 kJ mol^{-1}) results from the W1U value (−256.2 kJ mol^{-1}) is found in this case (13.6 kJ mol^{-1}). In general, the G2 method overestimates the exothermicity of $\Delta_f H^{298.15K}$.

Although the experimental heat of formation is still unknown for ClSO radical, a combination of the well-known experimental heat of formation data with our accurate W1U result can provide a possibility for its estimation. First of all, W1U reaction enthalpy, $\Delta_r H^{298.15K}_{W1U}$, can be calculated for the following reaction

$$ClSO + HOO \rightarrow HCl + SO_3 \quad \Delta_r H^{298.15K}_{W1U} = 398.1 \text{ kJ mol}^{-1} \quad (7)$$

Because the experimental heats of formation are available with relatively small uncertainties for HOO radical, HCl,

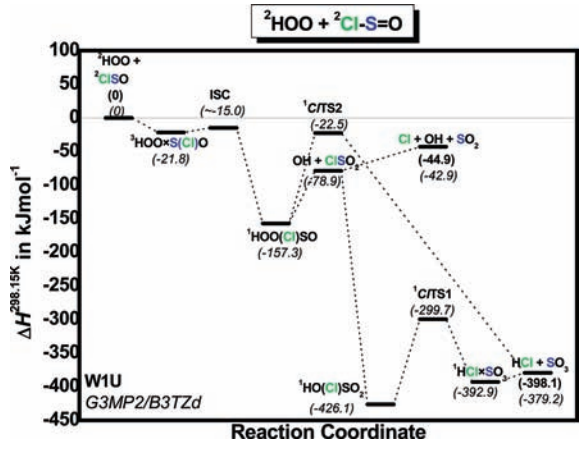

Figure 1. Enthalpy profile of the most important channel in the HOO + ClSO reaction system calculated using the G3MP2//B3TZd level of theory (italic). Available W1U energies are also given (bold).

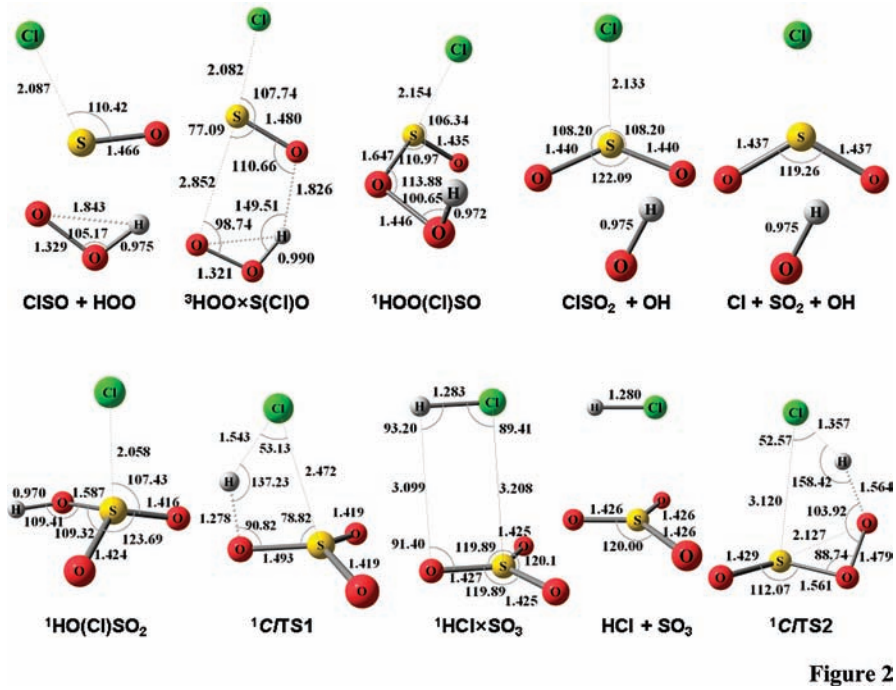

Figure 2. B3LYP/cc-pVTZ+d structures of the relevant stationary point on the potential energy surface of the HOO + ClSO reaction system.

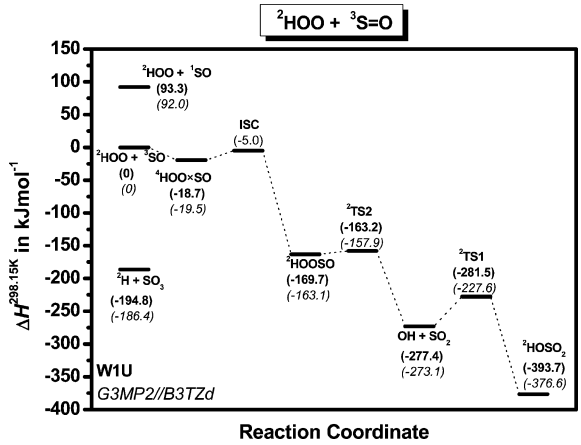

Figure 3. Relative enthalpy values (in kJ mol^{-1}) of relevant channel in the case of HOO + ^{3}SO reaction system calculated using W1U methods (bold). The G3MP2//B3TZd results are also shown (italic).

and SO_3 molecules (12.552, −92.31, and −395.753 kJ mol^{-1},[25] respectively), the heat of formation for ClSO is

$$\Delta_f H^{298.15K}_{theor}(ClSO) = \Delta_f H^{298.15K}_{exptl}(HCl) + \Delta_f H^{298.15K}_{exptl}(SO_3) - \Delta_f H^{298.15K}_{exptl}(HOO) - \Delta_r H^{298.15K}_{W1U}$$

$$\Delta_f H^{298.15K}_{theor}(ClSO) = 102.6 \text{ kJ mol}^{-1}$$

Dominant Channels. Both reaction systems exhibit a very large number of intermediate species on their complex potential surfaces, which are explored in detail. (See Figures S1-2 and Tables S1a,b in the Supporting Information.) Here only relatively low-lying and therefore kinetically important species are shown in Figures 1 and 2 for ClSO + HOO and in Figures 3 and 4 for ^{3}SO + HOO. The numeral assigned to the transition state (TSx) is the order of the energy level (e.g., TS1 is the lowest lying transition state on the given potential surface). The rotational constants and harmonic vibrational frequencies as well as the optimized geometries are listed for every species in Tables S3−S6 in the Supporting Information.

Reaction System of HOO and ClSO. The first possible step in the HOO + ClSO reaction system is a barrierless formation of a triplet van der Waals complex (vdW complex), ^{3}HOO × S(Cl)O, as shown in Figure 1. The geometrical parameters of the vdW complex seem to be very similar to those of the reactants, as presented in Figure 2. Note that the S−Cl bond (2.087 Å) in ClSO is close to the experimental values of the Cl_2SO species (2.074 Å).[26] In this planar complex (C_s symmetry), the terminal oxygen of the hydroperoxyl radical is orientated 2.852 Å away from the S atom of the S−O bond. The hydrogen is very close (1.826 Å) to the oxygen of the ClSO residue, which explains the stability of the complex (−21.8 kJ mol^{-1}) related to the enthalpy level of the reactants. The singlet state of the van der Waals complex was also calculated, but its enthalpy is found to be above the level of the reactants; therefore, it is excluded from further discussion because of its small stability.

Another possible channel is the abstraction of the hydrogen atom from the hydroperoxyl radical, but the barrier height seems to be high (73.0 kJ mol^{-1}), so it is a minor channel compared with the vdW-complex formation reaction. Consequently, this channel is also neglected from further discussions. Therefore, the unpaired spins of the vdW complex recombine via ISC to form the HOO(Cl)SO species, as presented in Figure 1. The relevant difference in enthalpy (−135.5 kJ mol^{-1}) could be caused by the formed O−S bond (1.647 Å). The orientation of the HOO is also changed significantly, and the O−O bond is expanded in the HOO(Cl)SO molecule (1.446 Å) compared with the vdW complex (1.321 Å). Consequently, the dissociation of hydroxyl radical may be the lowest-lying reaction channel. However, the dissociation enthalpy of HOO(Cl)SO to $ClSO_2$ and OH radicals through a loose transition state seems to be high (78.4 kJ mol^{-1}), but it is still under the enthalpy level of the entrance channel with a value of 78.9 kJ mol^{-1}. Another

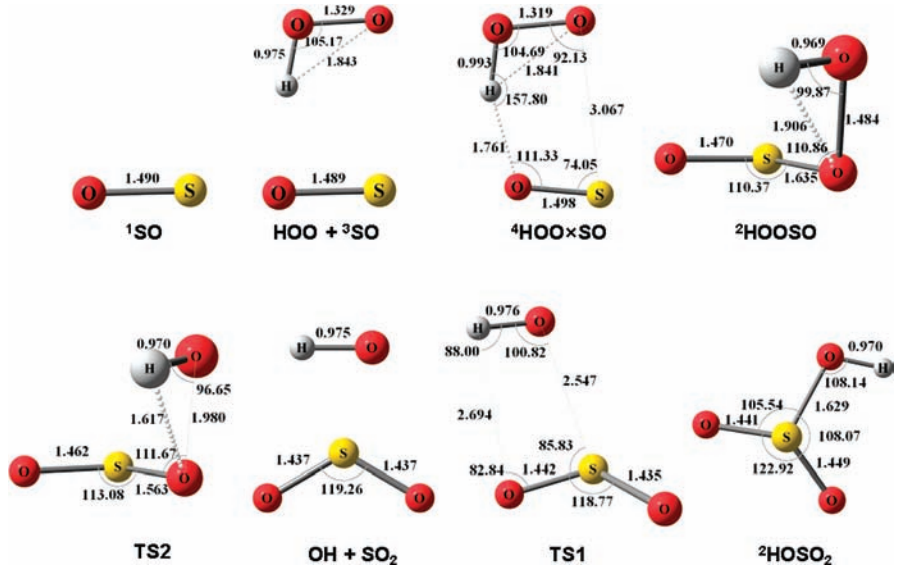

Figure 4. B3LYP/cc-pVTZ+d structures of the important stationary points on potential energy surface of the HOO + ^{3}SO.

TABLE 3: Standard Thermochemical Properties of Initial, Transition, Intermediate, and Final States for the Reaction of the HOO + ClSO[a]

	$S^{298.15K}$	ΔE_{rel} kJ mol^{-1}		$\Delta H^{298.15K}$ kJ mol^{-1}		$\Delta G^{298.15K}$ kJ mol^{-1}	
HOO + ClSO →	J mol^{-1} K^{-1}	A	B	A	B	A	B
^{2}HOO$^+$	228.8						
^{2}ClSO	279.0	0.0	0.0	0.0	0.0	0.0	0.0
^{3}HOO × S(Cl)O	372.8	−21.3		−21.8		18.5	(−)
^{1}HOO(Cl)SO	330.5	−154.0		−157.3		−104.5	
^{2}OH$^+$	178.2						
^{2}ClSO$_2$	299.5	−79.7		−78.9		−69.9	
^{2}Cl$^+$	158.8						
^{1}SO$_2$$^+$	248.2						
^{2}OH	178.2	−46.6	−48.6	−42.9	−44.9	−66.0	−68.0
HO(Cl)SO$_2$	311.1	−420.6		−426.1		−367.5	
^{1}*Cl*TS1	311.6	−293.6		−299.7		−241.2	
^{1}HCl × SO$_3$	367.5	−392.5		−392.9		−351.1	
^{1}HCl$^+$	186.5						
^{1}SO$_3$	262.6	−377.9	−396.8	−379.2	−398.1	−361.7	−380.6
^{1}*Cl*TS2	331.4	−18.5		−22.5		30.1	

[a] A: G3MP2//B3TZd; B: W1U levels of theory. Superscripts stand for the multiplicity of the species.

potential channel is the HCl elimination reaction, which might take place on a relatively high-lying, tight *Cl*TS2 transition state. (See Figure 1 and Table 3.) The entropy difference between *Cl*TS2 and OH + ClSO$_2$ is 146.3 J mol^{-1} K^{-1}, and the enthalpy of the loose transition state is reasonably lower-lying compared with *Cl*TS2 (56.4 kJ mol^{-1}). Accordingly, the dissociation to OH and ClSO$_2$ can be the dominant channel. As one may see in Figure 2, the Cl−S bond (2.133 Å) seems to be longer in ClSO$_2$ compared with that in ClSO (2.087 Å), which shows its weakness. The small dissociation enthalpy (36.0 kJ mol^{-1}) also confirms this. Perhaps, the Cl atom formed can be responsible for further hydroperoxyl radical formation (via reactions 2 and 3). In this case, the relative W1U (−44.9 kJ mol^{-1}) and G3MP2//B3TZd (−42.9 kJ mol^{-1}) enthalpies are in quite good agreement with each other (Table 3). An alternative reaction channel is the recombination of OH and ClSO$_2$ to give HO(Cl)SO$_2$ molecule, which is actually the global minimum on this potential surface. Even though this bimolecular reaction is energetically preferable [$\Delta_r H^{298.15K}$= −347.2 kJ mol^{-1}], its rate depends on the concentration of the reactants as well as on other conditions (e.g., pressure). Only one additional low-lying reaction channel starts from the HO(Cl)SO$_2$, which is also a HCl elimination (*Cl*TS1). However, the G3MP2//B3TZd result shows that the activation enthalpy is relatively high (126.4 kJ mol^{-1}). Interestingly enough, a product complex (HCl × SO$_3$) can also be formed in this reaction. The stabilization enthalpy is 13.7 kJ mol^{-1} relative to the product level (HCl + SO$_3$). Geometrical parameters and rotational constants of this complex were also characterized by microwave spectroscopy.[27] The distance of S and Cl was found to be 3.133 Å, which is in good agreement with our calculated result (3.208 Å).

Reaction System of HOO and ^{3}SO. As one can see in Figure 3, the triplet electronic state of the sulfur monoxide, ^{3}SO, is the ground state, which is more stable by 93.3 kJ mol^{-1} compared with its singlet state; however, the two S−O bond lengths do not significantly differ from each other (Figure 4). The H-abstraction reaction from HOO by ^{3}SO is unfavored because of its high barrier height (66.6 kJ mol^{-1} using the W1U method; more details in the Supporting Information). Consequently, the reactants can be stabilized only via a barrierless vdW-complex formation reaction (^{4}HOO × SO). In the quartet vdW complex, the geometrical

TABLE 4: Standard Thermochemical Properties of Initial, Transition, Intermediate, and Final States for the Reaction of the HOO + ^{3}SO[a]

	$S^{298.15K}$	ΔE_{rel} kJ mol^{-1}		$\Delta H^{298.15K}$ kJ mol^{-1}		$\Delta G^{298.15K}$ kJ mol^{-1}	
HOO + SO →	J mol^{-1} K^{-1}	A	B	A	B	A	B
^{2}HOO$^+$	228.8						
^{1}SO	212.7	92.0	93.3	92.0	93.3	94.7	96.0
^{2}HOO	228.8						
^{3}SO	221.8	0.0	0.0	0.0	0.0	0.0	0.0
^{4}HOO × SO	331.0	−18.0	−17.8	−19.6	−18.7	16.1	17.0
^{2}HOOSO	305.1	−160.0	−166.5	−163.1	−169.7	−119.7	−126.3
^{2}TS2	303.3	−154.4	−159.7	−157.9	−163.2	−114.0	−119.2
^{2}OH$^+$	178.2						
^{1}SO$_2$	248.2	−273.6	−277.9	−273.1	−277.4	−265.8	−270.2
^{2}TS1	320.8	−225.6	−279.4	−227.6	−281.5	−188.9	−242.7
^{2}HOSO$_2$	288.8	−371.4	−388.6	−376.6	−393.7	−328.3	−345.5

[a] A: G3MP2//B3TZd; B: W1U levels of theory. Superscripts stand for the multiplicity of the species.

parameters of HOO and ^{3}SO residues are close to those of the reactants, as may be seen in Figure 4. The O−O bond of the hydroperoxyl radical is parallel to the SO bond involving a 3.067 Å separation, and the hydrogen is orientated close to the SO oxygen (1.761 Å). The complex stabilization energy is about −19 kJ mol^{-1} (−18.7 and −19.5 kJ mol^{-1} calculated using W1U and G3MP2//B3TZd methods, respectively). The transition from the vdW complex to the ^{2}HOOSO species involves an ISC, where the quartet surface crossed the doublet one. The energy level of the formed ^{2}HOOSO species is lower, with −169.7 kJ mol^{-1} compared with the vdW complex. If one compares the structure of a ^{2}HOOSO radical with the vdW complex, as shown in the Figure 4, only two bond parameters are significantly changed: the distance between the sulfur and the terminal oxygen of the HOO radical (from 3.067 to 1.635 Å) and the distance between the two oxygens in the hydroperoxyl group (from 1.319 to 1.484 Å). The latter deviation can indicate the favored forward reaction, which is the dissociation via a low-lying transition state (TS2) to hydroxyl radical and sulfur dioxide. The activation enthalpy of TS2 is only 6.5 kJ mol^{-1} (W1U) with respect to the level of the ^{2}HOOSO (−169.7 kJ mol^{-1}). Furthermore, depending on the reaction condition (e.g., the concentration of the OH and SO_2 as well as the pressure), the OH + SO_2 products can form ^{2}HOSO$_2$. For the OH addition to SO_2 (TS1), the W1U method predicts a nearly barrierless reaction because a negative barrier height was found here (−4.1 kJ mol^{-1}). In contrast with this, the activation enthalpy of TS1 is estimated to be high by G3MP2//B3TZd method (45.5 kJ mol^{-1}). The ^{2}HOSO$_2$ species is the global minimum on the ^{2}HSO$_3$ potential energy surface ($\Delta H_{rel}^{298.15K}$ = −393.7 kJ mol^{-1}). The standard thermochemical properties of the above-mentioned molecules and transition states are collected in Table 4.

Role of the van der Waals Complexes. As was mentioned before, the reactants can be stabilized via barrierless vdW-complex formation reactions in both systems studied theoretically in this work. These stabilization enthalpies of prereactant complexes are about 20 kJ mol^{-1}. Note that a similar stabilization of the prereaction complex was also found in the H-abstraction reaction of OOH with unsaturated hydrocarbons.[28] This similarity tells us that the stabilization may be due to the $\pi-\pi$ interaction between the bonds of O−O and S−O as well as the H bonding. In these systems, the key reactions may proceed in all cases via vdW-complex formation, which is responsible for the possible low-lying transition to the adduct formation as well as for the ability of subsequent fast reactions.

4. Conclusions

Reactions of HO_2 radical with ClSO as well as SO were studied using the G3MP2//B3LYP/cc-pVTZ+d level of theory as well as the W1U method. The following mechanisms were supposed to be the main reaction channels

$$HO_2 + ClSO \rightarrow {}^3HOO \times S(Cl)O \rightarrow HOO(Cl)SO \rightarrow HO + ClSO_2 \rightarrow HO + Cl + SO_2$$

$$HO_2 + ClSO \rightarrow {}^3HOO \times S(Cl)O \rightarrow HOO(Cl)SO \rightarrow HO + ClSO_2 \rightarrow HO(Cl)SO_2$$

$$HO_2 + {}^3SO \rightarrow {}^4HOO \times SO \rightarrow {}^2HOOSO \rightarrow HO + SO_2$$

In both reaction mechanisms, the first step is a barrierless formation of relatively stable van der Waals complexes, which lead to the formation of intermediate adducts via ISC. Thermodynamically favored decomposition of HOOSO product results in OH radical and SO_2. In the case of ClSO and HO_2 reaction, after dissociation of OH from HOO(Cl)SO, OH addition reaction to $ClSO_2$ (resulted $HO(Cl)SO_2$) competes with further decomposition of $ClSO_2$ to Cl atom and SO_2. Cl atoms and OH radicals formed this way are able to generate further HO_2 via Cl + $CH_3OH \rightarrow CH_2OH$ + HCl and OH + $CH_3OH \rightarrow CH_2OH + H_2O$, followed by $CH_2OH + O_2 \rightarrow CH_2O + HO_2$. However, the formation of $HO(Cl)SO_2$ can be preferred in the high-pressure regime. Therefore, the theoretical results obtained in this part of the work support very well the experimental observations of secondary CH_2O formations following the Cl_2SO photolysis in the presence of CH_3OH and O_2 as well as the observed dependence on the experimental conditions. Heats of formation of ^{2}HSO$_3$, ^{2}HOOSO, and ^{2}OOS(H)O as well as ClSO radicals were also estimated using high-level quantum chemical calculations.

Acknowledgment. We thank M. Labadi for excellent technical support. We are also grateful to HPC Szeged for the computer facility. We thank the French Ministry of Foreign and European Affairs for financial support through the ECO-NET program.

Supporting Information Available: For both reaction systems, entire enthalpy profiles, Cartesian coordinates, corresponding harmonic frequencies, and all thermochemical properties belonging to all species studied as well as spin contami-

nations for the radical species. This material is available free of charge via the Internet at http://pubs.acs.org.

References and Notes

(1) Dréan, P.; Lemoine, B.; Devolder, P.; Schoemaecker, C.; Fittschen, C. *Int. J. Chem. Kinet*., submitted.

(2) Kawasaki, M.; Kasatani, K.; Sato, H.; Shinohara, H.; Nishi, N.; Ohtoshi, H.; Tanaka, I. *Chem. Phys.* **1984**, *91*, 285–291.

(3) Baum, G.; Effenhauser, C. S.; Felder, P.; Huber, J. R. *J. Phys. Chem.* **1992**, *96*, 756–764.

(4) Wang, H.; Chen, X.; Weiner, B. R. *J. Phys. Chem.* **1993**, *97*, 12260–12268.

(5) Maul, C.; Gericke, K.-H. *J. Phys. Chem. A* **2000**, *104*, 2531–2541.

(6) Roth, M.; Maul, C.; Gericke, K.-H. *Phys. Chem. Chem. Phys.* **2002**, *4*, 2932–2940.

(7) Chichinin, A.; Einfeld, T. S.; Gericke, K.-H.; Grunenberg, J.; Maul, C.; Schäfer, L. V. *Phys. Chem. Chem. Phys.* **2005**, *7*, 301–309.

(8) Chu, L.-K.; Lee, Y.-P.; Jiang, E. Y. *J. Chem. Phys.* **2004**, *120*, 3179–3184.

(9) Roth, M.; Maul, C.; Gericke, K.-H. *Phys. Chem. Chem. Phys.* **2002**, *4*, 2932–2940.

(10) Atkinson, R.; Baulch, D. L.; Cox, R. A.; Crowley, J. N.; Hampson, R. F.; Hynes, R. G.; Jenkin, M. E.; Rossi, M. J.; Troe, J. *Atmos. Chem. Phys.* **2006**, *6*, 3625–4055.

(11) Stephens, P. J.; Devlin, F. J.; Chabalowski, C. F.; Frisch, M. J. *J. Phys. Chem.* **1994**, *45*, 11623–11627.

(12) Poater, J.; Solá, M.; Duran, M.; Roblesy, J. *Phys. Chem. Chem. Phys.* **2002**, *4*, 722–731.

(13) Dunning, T. H. *J. Chem. Phys.* **1989**, *90*, 1007–1023.

(14) Baboul, A. G.; Curtiss, L. A.; Redfern, P. C.; Raghavachari, K. *J. Chem. Phys.* **1999**, *110*, 7650.

(15) Martin, J. M. L.; de Oliveira, G. *J. Chem. Phys.* **1999**, *111*, 1843–1856.

(16) Parthiban, S.; Martin, J. M. L. *J. Chem. Phys.* **2001**, *114*, 6014–6029.

(17) Frisch, M. J. ; Trucks, G. W.; Schlegel, H. B.; Scuseria, G. E.; Robb, M. A.; Cheeseman, J. R.; Montgomery, Jr., J. A.; Vreven, T.; Kudin, K. N.; Burant, J. C.; Millam, J. M.; Iyengar, S. S.; Tomasi, J.; Barone, V.; Mennucci, B.; Cossi, M.; Scalmani, G.; Rega, N.; Petersson, G. A.; Nakatsuji, H.; Hada, M.; Ehara, M.; Toyota, K.; Fukuda, R.; Hasegawa, J.; Ishida, M.; Nakajima, T.; Honda, Y.; Kitao, O.; Nakai, H.; Klene, M.; Li, X.; Knox, J. E.; Hratchian, H. P.; Cross, J. B.; Bakken, V.; Adamo, C.; Jaramillo, J.; Gomperts, R.; Stratmann, R. E.; Yazyev, O.; Austin, A. J.; Cammi, R.; Pomelli, C.; Ochterski, J. W.; Ayala, P. Y.; Morokuma, K.; Voth, G. A.; Salvador, P.; Dannenberg, J. J.; Zakrzewski, V. G.; Dapprich, S.; Daniels, A. D.; Strain, M. C.; Farkas, O.; Malick, D. K.; Rabuck, A. D.; Raghavachari, K.; Foresman, J. B.; Ortiz, J. V.; Cui, Q.; Baboul, A. G.; Clifford, S.; Cioslowski, J.; Stefanov, B. B.; Liu, G.; Liashenko, A.; Piskorz, P.; Komaromi, I.; Martin, R. L.; Fox, D. J.; Keith, T.; Al-Laham, M. A.; Peng, C. Y.; Nanayakkara, A.; Challacombe, M.; Gill, P. M. W.; Johnson, B.; Chen, W.; Wong, M. W.; Gonzalez, C.; Pople, J. A. *Gaussian 03*, revision D.02; Gaussian, Inc.: Wallingford, CT, 2004.

(18) Klopper, W.; Tew, D. P.; González-García, N.; Olzmann, M. *J. Chem. Phys.* **2008**, *129*, 114308–114314.

(19) Blitz, M. A.; Hughes, K. J.; Pilling, M. J. *J. Phys. Chem. A* **2003**, *107*, 1971–1978.

(20) Somnitz, H. *Phys. Chem. Chem. Phys.* **2004**, *6*, 3844–3851.

(21) Fulle, D.; Hamann, H. F.; Hippler, H. *Phys. Chem. Chem. Phys.* **1999**, *1*, 2695–2702.

(22) Li, W. K.; McKee, M. L. *J. Phys. Chem. A* **1997**, *101*, 9778–9782.

(23) Curtiss, L. A.; Redfern, P. C.; Raghavachari, K.; Pople, J. A. *J. Chem. Phys.* **2001**, *114*, 108–117.

(24) Parthiban, S.; Martin, J. M. L. *J. Chem. Phys.* **2001**, *114*, 6014–6029.

(25) Alexander Burcat and Branko Ruscic Ideal Gas Thermochemical Database with updates from Active Thermochemical Tables. ftp://ftp.technion.ac.il/pub/supported/aetdd/thermodynamics (accessed July 23, 2007). Mirrored at http://garfield.chem.elte.hu/Burcat/burcat.html (accessed July 23, 2007).

(26) Mata, F.; Carballo, N. *J. Mol. Struct.* **1983**, *101*, 233–238.

(27) Canagaratna, M.; Phillips, J. A.; Goodfriend, H.; Fiacco, D. L.; Ott, M. E.; Harms, B.; Leopold, K. R. *J. Mol. Spectrosc.* **1998**, *192*, 338–347.

(28) Szori, M.; Abou-Abdo, T.; Fittschen, C.; Csizmadia, I. G.; Viskolcz, B. *Phys. Chem. Chem. Phys.* **2007**, *9*, 1931–1940.

JP901183K